# Characterization of self-asembly and evolution in carbon nanotube thin film field emitter

**Sinha, N., Mahapatra, R., Yeow, J.T.W., Melnik, R.V.N. and Jaffray, D.A.**

**IEEE Nano 2006 - Proc. of the 6th IEEE International Conference on Nanotechnology, Cincinnati, OH, USA, July 16-20, 2006, IEEE Proceedings, 1-4244-0078-3/06, 4 pages, 2006**

# Characterization of Self-Assembly and Evolution in Carbon Nanotube Thin Film Field Emitter

N. Sinha[a], D. Roy Mahapatra[b], J.T.W. Yeow[a*1], R.V.N. Melnik[b] and D.A. Jaffray[c]

[a]*Department of Systems Design Engineering, University of Waterloo, ON, N2L3G1, Canada*
[b]*Mathematical Modeling and Computational Sciences, Wilfrid Laurier University, Waterloo, ON, N2L3C5, Canada*
[c]*Department of Radiation Physics, Princess Margaret Hospital, University Health Network, Toronto, ON, M5G2M9, Canada*

## Abstract

**Carbon nanotubes (CNTs) are found to be good sources of cold cathode electron for a variety of technological applications. In this paper, we analyze the evolution and self-assembly of randomly oriented CNTs in a thin film during field emission under diode configuration. A model of the evolution of CNT thin film is proposed, where the CNTs are assumed to decay by fragmentation and formation of plasma consisting of carbon atoms and impurities. The random orientation of the CNTs and the electrodynamic interaction among themselves are modeled to explain the self-assembly caused by dynamic reorientation of the CNTs. Finally, the nucleation coupled degradation model and the electrodynamic forcing model are employed to estimate the current-voltage characteristics based on the modified Fowler-Nordheim equation for field emission. The simulated results are in close agreement with the experimental results.**

**Keywords :** Field emission, carbon nanotube array, evolution, electrodynamic, self-assembly.

## I. Introduction

Carbon nanotubes (CNTs) are among the best field emitters, and their application in field emission devices, such as field emission displays, x-ray tube sources, electron microscopes, cathode-ray lamps, and nanolithography systems are under active research [1]-[5]. CNTs have remarkable properties such as low voltage operation, good emission ability and low energy spread. These field emission properties are attributed to their structural integrity, high thermal conductivity, chemical stability, high aspect ratio and their capability to generate a large electric field enhancement in order to obtain electron emission at low electric fields. The most important requirement of CNT cathodes in field emission devices is to have stable field-emission current densities without compromising the lifetime of the device. In order to improve the device performance, the electrical failure mechanisms of CNT cathodes and subsequent effect on the current-voltage characteristics must be understood. Such studies are not available in published literature. In this paper we address some of the related problems, which, to these author's knowledge, have direct consequence on the device performance.

Several studies have reported experimental observations in favour of the degradation and failure of CNT cathodes. These studies can divided into two categories: (1) studies related to degradation of single nanotube emitter [6] and (2) studies related to degradation of CNT thin films [7]. Although the mode of degradation and failure of single nanotube emitters can either be abrupt or gradual, degradation of a thin film emitter is always gradual [8]. The gradual degradation occurs either during initial current-voltage measurement or during measurements at constant applied voltage over a long period of time. Nevertheless, it can be concluded that the gradual degradation of thin films occurs due to the failure of individual emitters. Up to date, most of the studies have focused on single nanotube emitters. Although some studies have reported experimental observations for thin films, from mathematical and computational view points, the detailed models and characterization methods are available only for vertically aligned CNTs grown on patterned surface [9], [10]. In a CNT film, the array of CNTs may ideally be aligned vertically. However, in that case it is desired that the individual CNTs are evenly separated in such a way that their spacing is greater than their height to minimize the screening effect. As a trade off, in the latter case, the emission properties as well as the lifetime of cathodes are adversely affected, which are due to the significant reduction in density of CNTs. On the other hand, for the cathodes with randomly oriented CNTs, the field emission current is produced by two types of sources: (i) small fraction of CNTs that point toward the current collector (anode) and (ii) oriented CNTs subjected to electrodynamic forcing causing reorientation due to the curved and flexible nature of CNTs. The advantage of this type of cathode is that always a large number of CNTs take part in the field emission over a longer period of time, which is unlikely in case uniformly alligned CNTs. Due to this reason, thin film of randomly oriented CNTs have been considered in the present study. Although some preliminary work has been reported in [11], no detailed model and subsequent characterization method are available for thin films, where the array of CNTs may undergo incredibly complex dynamics during the process of charge transport over time. In the majority of analytical and design studies, it is usual practice to employ the classical Fowler-Nordheim equation [12] for field emission from metallic surface with correction factors to deal with the CNT tip geometry etc. Such an empirical approach applies only to individual type samples (e.g. CNT geometry, method of preparation, CNT density, diode configuration etc.) and also to a particular range of applied voltage. Also, in order to account for the oriented CNTs and interaction between themselves, it is necessary to consider the space charge and the electrodynamic forces responsible for realignment. Some of the related factors are also important from device design considerations.

By taking into account the evolution of CNT array, a

[1]Corresponding author: JTWY e-mail: jyeow@engmail.uwaterloo.ca



1-4244-0078-3/06/$20.00 (c) 2006 IEEE

model has been developed in this paper. The homogeneous nucleation rate is coupled to a moment model to calculate the concentration of carbon cluster due to the decay of CNTs over time. This information is then used in time-incremental manner to describe the evolved state of the CNTs in representative volume element. Finally, the current density is calculated by plugging the values of the tube orientation angle and the effective electric field in the modified Fowler-Nordheim equation. Diode current is then computed by integrating this current density over the anode area.

The CNT film under study in this work consists of randomly oriented multi-walled nanotubes (MWNTs). The film is grown on a stainless steel surface. The film has a surface area of 1 $\mathrm{cm}^2$ and thickness of $20-30$ $\mu$m. The anode consists of a 1.59 mm thick copper plate with an area of 49.93 $\mathrm{mm}^2$. Current-voltage characteristics have been measured over a range of DC voltage for a controlled gap between the cathode and the anode.

## II. Model formulation

Let $N_T$ be the total number of carbon atoms in the representative volume element ($V_{\mathrm{cell}}$) of the thin film, $N(t)$ be the number of CNTs in the film, and $N_{\mathrm{CNT}}(t)$ is total number of carbon atoms present in the tube. Hence,

$$N_T = N(t)N_{CNT}(t) + N_{\mathrm{plasma}} \tag{1}$$

where $N_{\mathrm{plasma}}$ is the total number of carbon atoms in the plasma at time $t$ and is given by

$$N_{\mathrm{plasma}} = V_{\mathrm{cell}} \int_0^t dn_1(t) \tag{2}$$

where $n_1$ is the monomer concentration (unit in $(m^{-3})$) of carbon and $V_{\mathrm{cell}}$ is the cell volume in $(\mathrm{m}^3)$. Therefore, by combining Eqs. (1) and (2) one can write

$$N(t) = \frac{1}{N_{CNT}(t)}\left[N_T - V_{\mathrm{cell}} \int_0^t dn_1(t)\right] \tag{3}$$

In order to determine $n_1(t)$, we introduce the nucleation coupled model [13], [14]. Here, we modify this model according to the problem in hand. The evolution equations are expressed as

$$\frac{dN_{\mathrm{kin}}}{dt} = J_{\mathrm{kin}} \tag{4}$$

$$\frac{dS}{dt} = -\frac{J_{\mathrm{kin}} S g^*}{n_1} - (S-1)\frac{B_1 A_n}{2v_1} \tag{5}$$

$$\frac{dM_1}{dt} = J_{\mathrm{kin}} d_p^* + (S-1)B_1 N_{\mathrm{kin}} \tag{6}$$

$$\frac{dA_n}{dt} = \frac{J_{\mathrm{kin}} S g^{*2/3} s_1}{n_1} + \frac{2\pi B_1 S(S-1)M_1}{n_1} \tag{7}$$

where $N_{\mathrm{kin}}$ is the kinetic normalization constant, $J_{\mathrm{kin}}$ is the kinetic nucleation rate, $S$ is the saturation ratio, $g^*$ is the critical cluster size, $A_n$ is the total surface area of stable plasma $(\mathrm{m}^2)$, $v_1$ is monomer volume $(\mathrm{m}^3)$, $M_1$ is the moment of cluster size distribution, $d_p^*$ is the diameter of the particle of critical cluster $(\mathrm{m})$, and $s_1$ is the surface area of a monomer $(\mathrm{m}^2)$. The quantities $S$, $N_{\mathrm{kin}}$, $J_{\mathrm{kin}}$, $g^*$, $B_1$, and $M_1$ are defined as

$$S = \frac{n_1}{n_s} \tag{8}$$

$$N_{\mathrm{kin}} = \frac{n_1}{S}\exp(\Theta) \tag{9}$$

$$J_{\mathrm{kin}} = \frac{\beta_{ij} n_1^2}{12S}\sqrt{\frac{\Theta}{2\pi}}\exp\left(\Theta - \frac{4\Theta^3}{27(\ln S)^2}\right) \tag{10}$$

$$g^* = \left(\frac{2}{3}\frac{\Theta}{\ln S}\right)^3 \tag{11}$$

$$B_1 = 2n_s v_1 \sqrt{\frac{kT}{2\pi m_1}} \tag{12}$$

$$M_1 = \int_{d_p^*}^{d_p^{\max}} \Big(n(d_p,t)d_p\Big)d(d_p) \tag{13}$$

where $n_s$ is the equilibrium saturation monomer concentration $(\mathrm{m}^{-3})$, $\Theta$ is the dimensionless surface tension, $\beta_{ij}$ is the collision frequency function for collisions between $i$-mers and $j$-mers, $k$ is the Boltzmann's constant $(\mathrm{J/K})$, $T$ is the temperature $(\mathrm{K})$, $m_1$ is the mass of monomer $(\mathrm{Kg})$, $d_p$ is the particle diameter $(\mathrm{m})$, $d_p^{\max}$ is the maximum diameter of the particle $(\mathrm{m})$, and $n(d_p,t)$ is particle size distribution function. The quantities $\beta_{ij}$ and $\Theta$ are defined as [15]

$$\beta_{ij} = \left(\frac{3v_1}{4\pi}\right)^{1/6}\sqrt{\frac{6kT}{\rho_p}\left(\frac{1}{i}+\frac{1}{j}\right)}\left(i^{1/3}+j^{1/3}\right)^2 \tag{14}$$

$$\Theta = \frac{\sigma s_1}{kT} \tag{15}$$

where $\rho_p$ is particle mass density $(\mathrm{Kg/m}^3)$ and $\sigma$ is the surface tension $(\mathrm{N/m})$. Equations (4)-(7) form a set of four nonlinear coupled ordinary differential equations, which describe the time evolution of plasma from the CNTs. These nonlinear equations are solved in $(n_1, S, M_1, A_n)$ using a finite difference scheme. At $t=0$, the CNTs are assumed to be randomly oriented. This random distribution is parameterized in terms of the upper bound of the CNT tip deflection which is given by $\Delta x_{\max} = h/q$, where $h$ is the CNT length and $q$ is an integer number. At $t \leftarrow t + \Delta t$, the computed value of $n_1(t)$, the geometrical quantities of the CNTs, and the tip angles are plugged in the Fowler-Nordheim equation to calculate the current density.

The electric field along the tube axis at the CNT tip is given by

$$E(x,y)_{z'} = \sqrt{1 - \frac{x^2+y^2}{R^2}}\frac{(h_0 - v_{\mathrm{burn}}t)E_{tip}}{(d - h_0 + v_{\mathrm{burn}}t)} \tag{16}$$

where $R$ is one-half of the spacing between two adjacent CNTs, $h_0$ is the initial height of CNTs, $v_{\mathrm{burn}}$ is the burning rate, or the rate of decrease in CNT length, $E_{\mathrm{tip}} = V/d$ is the background electric field at the tip of each CNTs, and $d$ is the distance between the cathode substrate and the anode, that is, the electrode gap under diode configuration, as shown in Fig. 1. The burning rate $v_{\mathrm{burn}}$ is of the form

$$v_{\mathrm{burn}} = V_{\mathrm{cell}}\frac{dn_1(t)}{dt}\left[\frac{s(s-a_1)(s-a_2)(s-a_3)}{n^2a_1^2 + m^2a_2^2 + nm(a_1^2+a_2^2-a_3^2)}\right]^{1/2} \tag{17}$$

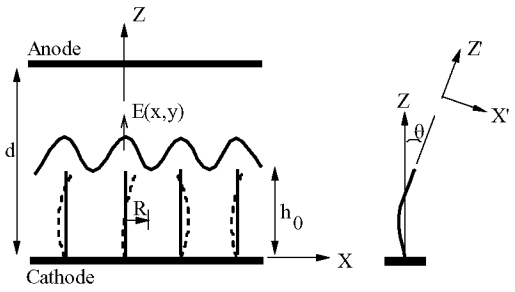


Fig. 1. CNT array configuration

where $a_1$, $a_2$, $a_3$ are lattice constants, $s = \frac{1}{2}(a_1 + a_2 + a_3)$, and $(n, m)$ is an integer pair (see [16]). The effective electric field for field emission calculation is given by

$$E(t)_z = E(x, y)_{z'} \cos(\theta(t)) \tag{18}$$

where $\theta$ is the angle that a nanotube makes with the $Z$-axis as shown in Fig. 1. The orientation angle $\theta$ is coupled with the electrodynamic forces through the mechanics of deformation of the CNT as an one-dimensional nano-wire. We omit the related details of the formulation here. Instead, here we consider the Cartesian components of Lorentz force acting on the each of the CNT tip to demsonstrate the preliminary calculation procedure. The force components (see [17] for details) along z and x directions are expressed as

$$f_z = \pi d_t e \hat{n}_0 E_{\text{tip}} \cos\theta \tag{19}$$

$$f_x = \pi d_t e \hat{n}_0 E_{\text{tip}} \cos\theta \sin\theta \tag{20}$$

where $d_t$ is the diameter of the tube, $e$ is the electronic charge, and $\hat{n}_0$ is the CNT tube surface electron density corresponding to the Fermi level energy. $\hat{n}_0$ is expressed as

$$\hat{n}_0 = \frac{kT}{\pi b^2 \Delta} \tag{21}$$

where $b$ is is interatomic distance and $\Delta$ is the overlap integral ($\approx 2eV$ for carbon). The current density is calculated by substituting the value of $E(t)_z$ in the modified Fowler-Nordheim equation

$$J = \frac{BE(t)_z^2}{\Phi} \exp\left( - \frac{C\Phi^{3/2}}{E(t)_z} \right) \tag{22}$$

where $\Phi$ is the work function (eV) for the CNT tip, and B and C are constants.

## III. Results and Discussions

The first step in our computation is to obtain the value of $n_1$ (the carbon cluster concentration) at a given time step from the nucleation coupled model. In this paper, it has been assumed that at $t = 0$, the diode contains minimal amount of carbon cluster in plasma. The CNTs degrade over time (due to both fragmentation and self-assembly) and the carbon cluster concentration in each cell also changes accordingly. Based on this assumption, the initial condition was set as $n_1(0) = 100$, $S(0) = 100$, $M_1(0) = 2.12 \times 10^{-16}$, $A_n(0) = 0$, and $T = 303K$. Equations (4)-(7) were solved simultaneously to obtain $n_1$. Fig. 2 shows the $n_1(t)$ history over a small time duration ($160s$). Such evolution indicates that the rate of decay is very slow, which in turn implies longer lifetime of electrodes. However, a more detailed investigation on the physical mechanism of cluster formation at the CNT tips and fragmentation of the curved CNTs is necessary, which will be the topic of a forthcoming articles. It is obvious from Eq. (14) that the heterogeneous cluster dynamics will play important role, which in turn is likely to alter the space charge distribution and the ballistic transport properties of the gap region. A more accurate but intensive approach would be to obtain the current density at the anode by solving a quantum-hydrodynamic type problem for the gap region.

As discussed earlier, we use the computed values of $n_1(t)$ while evaluating the electric field in Eq. (16). At $t = 0$, we assign random orientation angles of CNTs. The angles are then used to calculate the component of electrodynamic forces. In the next time step, $t \leftarrow t + \Delta t$, we calculate the deformed state of the CNTs as function of the force components and update the tip angle of each CNTs. For a cell containing 100 CNTs, Fig. 3 shows the initial distribution ($t = 0$) and the terminal distribution ($t = 160s$ corresponding to Fig. 2) of the tip angles. The large fluctuation in the tip angles for certain CNTs can be attributed to the electrodynamic forcing.

The distribution of tip angles and the resulting electric field were plugged in Eq. (22) and the output current were obtained by integrating the current density $J$ over the anode surface. The constants B and C in Eq. (22) were taken as $B = (1.4 \times 10^{-6}) \times \exp((9.8929) \times \Phi^{-1/2})$ and $C = 6.5 \times 10^7$, respectively [18]. As reported in the literature, the work function $\Phi$ for CNTs is smaller than the work functions of metal, silicon, and graphite [18]. However, there are significant variations in the experimental values of $\Phi$ depending on the types of CNTs (SWNT or MWNT and even geometric parameters). In the present calculation, the value of work function was taken as 2.2 eV. The current-voltage (I-V) characteristics of the film for $61.9\mu$m gap is shown in Fig. 4. The two simulated curves in the figure correspond to the cases where the bounds of the initial tip deflections are small in one case ($\Delta x_{\max} = h_0/100$) and large in the other case ($\Delta x_{\max} = h_0/6$). It is clear from the comparison between simulated results in Fig. 4 that the output current is low for the sample with high average deflection, which is physically consistent. For the small angle case, the simulated I-V curve is in close agreement with the experimental curve. However, the deviation of the simulated result from experimental curves can be attributed to various approximations that were made in the model. Besides, the effects of Coulomb force and van der Waal force were not considered in the present simulation and this may be one of the important aspect to be analyzed next. Also, the mechanics of the CNTs as nano-wires and the quantum-hydrodynamic type treatment of the gap region are likely to be important aspects to be considered. A more detailed investigations including these aspects will be handled in the ongoing research effort.

## IV. Conclusion

In this paper, we have developed a computational model, which combines the nucleation coupled model of degradation

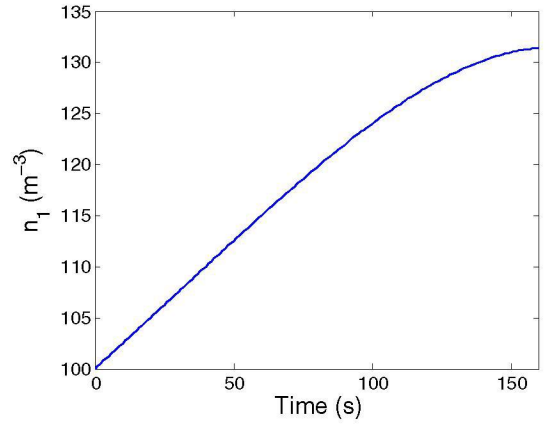


Fig. 2. Variation of the carbon cluster concentration with time. Initial condition: $n_1(0) = 100m^{-3}$, $S(0) = 100$, $T = 303K$, $M(0) = 0$.

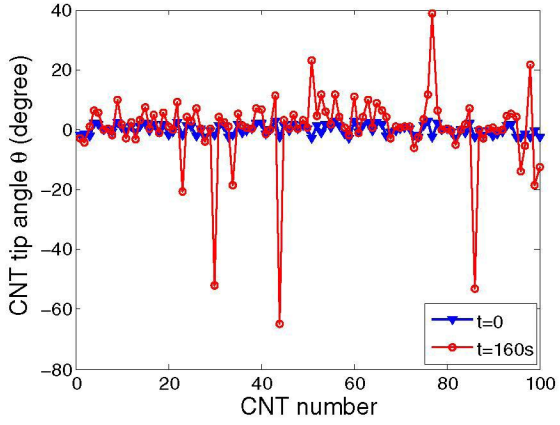


Fig. 3. Distribution of tip angles over the number of CNTs

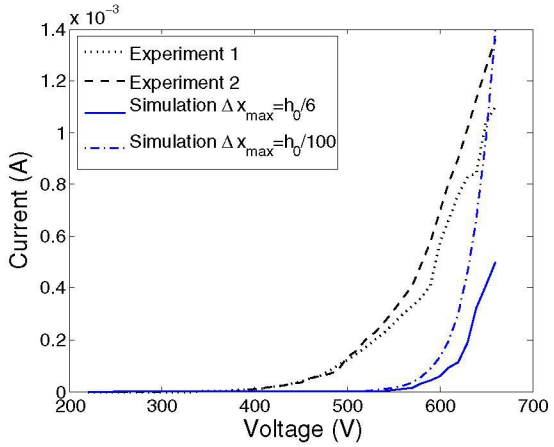


Fig. 4. Comparison of simulated current-voltage characteristics with experiments

of CNT films and electrodynamic forcing on randomly oriented CNTs. The model thus handles several complexities at the device scale, especially the evolution and self-assembly of the system of CNTs during field emission. The effects of these complexities on the I-V characteristics are indeed pronounced as clearly seen from the simulated results and a close agreement of these results with experiments. However, several other physical mechanisms, although well known in context of an isolated CNT but less known at the system level, need to be incorporate in the model in a consistent manner, so that the device performance can be analyzed and explained by comparing a range of experiments.

## Acknowledgement

This work was made possible by financial support from NSERC. MMO/EMK, University of Waterloo, and Princess Margaret Hospital, Toronto, Canada.

## References

[1] W. B. Choi, D. S. Chung, J. H. Kang, H. Y. Kim, Y. W. Jin, I. T. Han, Y. H. Lee, J. E. Jung, N. S. Lee, G. S. Park, and J. M. Kim, "Fully sealed, high-brightness carbon-nanotube field-emission display," *Appl. Phys. Lett.*, vol. 75, pp. 3129-3131, 1999.

[2] A. Okazaki, S. Akita, H. Nishijima, and Y. Nakayama, "Nanolithography of organic polysilane films using carbon nanotube tips," *Jpn. J. Appl. Phys.*, Part 1, vol. 39, no. 6B, pp. 3744-3746, 2000.

[3] J. M. Bonard, J. P. Salvetat, T. Stockli, L. Forro, and A. Chatelain, "Field emission from carbon nanotubes: perspectives for applications and clues to the emission mechanism," *Appl. Phys. A*, vol. 69, pp. 245-254, 1999.

[4] Y. Saito, and S. Uemura, "Field emission from carbon nanotubes and its application to electron sources," *Carbon*, vol. 38, pp. 169-182, 2000.

[5] H. Sugie, M. Tanemure, V. Filip, K. Iwata, K. Takahashi, and F. Okuyama, "Carbon nanotubes as electron source in an X-ray tube," *Appl. Phys. Lett.*, vol. 78, pp. 2578-2580, 2001.

[6] J. M. Bonard, F. Maier, T. Stockli, A. Chatelain, W. A. de Heer, J. P. Salvetat, and L. Forro, "Field emission properties of multiwalled carbon nanotubes," *Ultramicroscopy*, vol. 73, pp. 7-15, 1998.

[7] L. Nilsson, O. Groening, P. Groening, and L. Schlapbach, "Collective emission degradation behavior of carbon nanotube thin-film electron emitters," *Appl. Phys. Lett.*, vol. 79, pp. 1036-1038, 2001.

[8] J. M. Bonard, C. Klinke, K. A. Dean, and B. F. Coll, "Degradation and failure of carbon nanotube field emitters," *Phys. Rev. B*, vol. 67, no. 11, pp. 115406 (1-10), 2003.

[9] D. Nicolaescu, L. D. Filip, S. Kanemaru, and J. Itoh, "Modeling of optimized field emission nanotriodes with aligned carbon nanotubes of variable heights," *Jpn. J. Appl. Phys.*, vol. 43, no. 2, pp. 485-491, 2004.

[10] D. Nicolaescu, V. Filip, S. Kanemaru, and J. Itoh, "Modeling of field emission nanotriodes with carbon nanotube emitters, " *J. Vac. Sci. Technol.*, vol. 21, no. 1, pp. 366-374, 2003.

[11] N. Sinha, and J. T. W. Yeow, "Modeling of the behavior of random carbon nanotubes during field emission," *The 2005 Int. Conf. MEMS, Nano, Smart Sys.*, pp. 371-376, 2005.

[12] R.H. Fowler, and L. Nordheim, "Electron emission in intense electric field," *Proc. Royal Soc. London A*, vol. 119, pp. 173-181, 1928.

[13] S. K. Friedlander, "Dynamics of aerosol formation by chemical reactions," *Ann. N.Y. Acad. Sci.*, vol. 404, pp. 354-364, 1983.

[14] S. L. Grishick, C. P. Chiu, and P. H. McMurry, "Time-dependent aerosol models and homogeneous nucleation rates," *Aerosol Sci. Technol.*, vol. 13, pp. 465-477, 1990.

[15] S. K. Friedlander, *Smoke, Dust and Haze: Fundamentals of Aerosol Behavior*, New York: Wiley, 1977.

[16] H. Jiang, P. Zhang, B. Liu, Y. Huang, P. H. Geubelle, H. Gao, and K. C. Hwang, "The effect of nanotube radius on the constitutive model for carbon nanotubes," *Comp. Mat. Sci.*, vol. 28, pp. 429-442, 2003.

[17] G. Y. Slepyan, S. A. Maksimenko, A. Lakhtakia, O. Yevtushenko, and A. V. Gusakov, "Electrodynamics of carbon nanotubes: Dynamic conductivity, impedance boundary conditions, and surface wave propagation," *Phys. Rev. B*, vol. 60, no. 24, pp. 17136-17149, 1999.

[18] Z. P. Huang, Y. Tu, D. L. Carnahan, and Z. F. Ren, "Field emission of carbon nanotubes," *Encyl. Nanosci. Nanotechnol.* (Ed. H. S. Nalwa), vol. 3, pp. 401-416, 2004.